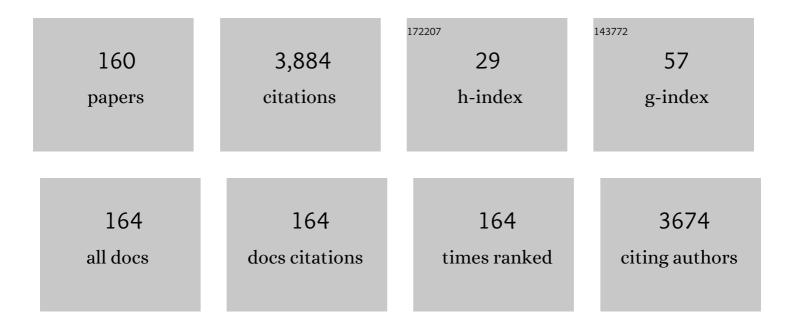
Takahisa Omata

List of Publications by Year in descending order

Source: https://exaly.com/author-pdf/5283826/publications.pdf Version: 2024-02-01



ΤΛΚΛΗΙΩΛ ΟΝΛΛΤΛ

#	Article	IF	CITATIONS
1	Proton-conducting phosphate glass: Recent development as an electrolyte in intermediate temperature fuel cells. Journal of the Ceramic Society of Japan, 2022, 130, 1-9.	O.5	5
2	Direct evaluation of hole effective mass of SnS–SnSe solid solutions with ARPES measurement. Physical Chemistry Chemical Physics, 2022, 24, 634-638.	1.3	6
3	Origin of the Temperature Dependence of Proton Conductivity in Phosphate Glass Prepared by Alkali-Proton Substitution Technique. Journal of the Electrochemical Society, 2022, 169, 034517.	1.3	1
4	Site-Dependent Tb ³⁺ Luminescence by Energy Transfer from Ce ³⁺ in Ce ³⁺ –Tb ³⁺ Codoped LaLuO ₃ . Journal of Physical Chemistry C, 2022, 126, 6499-6504.	1.5	6
5	Contribution of the Sn 5s state to the SnS valence band: direct observation via ARPES measurements. Electronic Structure, 2022, 4, 025004.	1.0	6
6	Growth of β-NaGaO ₂ thin films using ultrasonic spray pyrolysis. Journal of Asian Ceramic Societies, 2022, 10, 520-529.	1.0	3
7	Zn(Te1â^'Se) quantum dots synthesized through a facile route and their band-edge and surface state driven visible-light emission. Journal of Luminescence, 2021, 231, 117829.	1.5	5
8	Understanding the effect of oxide components on proton mobility in phosphate glasses using a statical analysis approach. RSC Advances, 2021, 11, 3012-3019.	1.7	6
9	SnS Homojunction Solar Cell with nâ€īype Single Crystal and pâ€īype Thin Film. Solar Rrl, 2021, 5, 2000708.	3.1	29
10	Enhanced Valley Splitting of Exciton Emission in Colloidal PbSe Quantum Dots When the Interdot Distance Coincides with Onset of Förster Resonance Energy Transfer. Journal of Physical Chemistry Letters, 2021, 12, 3120-3126.	2.1	2
11	White-light emission from zinc chalcogenide alloy quantum dots with gradient compositions. Journal of Luminescence, 2021, 232, 117876.	1.5	1
12	Investigating the role of GeO ₂ in enhancing the thermal stability and proton mobility of proton-conducting phosphate glasses. Journal of Materials Chemistry A, 2021, 9, 20595-20606.	5.2	6
13	First Principles Calculation of Electrical and Optical Properties of Cu ₃ AsO ₄ : Promising Thin-Film Solar Cell Absorber from Nonferrous Metal Manufacturing By-Products. Materials Transactions, 2021, , .	0.4	0
14	Anhydrous Silicophosphoric Acid Glass: Thermal Properties and Proton Conductivity. ChemPhysChem, 2021, , .	1.0	1
15	<mml:math xmlns:mml="http://www.w3.org/1998/Math/MathML"><mml:mi>n</mml:mi></mml:math> -type electrical conduction in SnS thin films. Physical Review Materials, 2021, 5, .	0.9	8
16	Surface modification of soda–lime–silicate glass via the high-temperature electrochemical injection of tin ions. Applied Surface Science, 2020, 532, 147421.	3.1	2
17	Fermi Energy Limitation at β-CuGaO ₂ Interfaces Induced by Electrochemical Oxidation/Reduction of Cu. ACS Applied Energy Materials, 2020, 3, 9117-9125.	2.5	5
18	Growth of Large Single Crystals of n-Type SnS from Halogen-Added Sn Flux. Crystal Growth and Design, 2020, 20, 5931-5939.	1.4	16

#	Article	IF	CITATIONS
19	Ultra-thin phosphate glass exhibiting high proton conductivity at intermediate temperatures. International Journal of Hydrogen Energy, 2020, 45, 16690-16697.	3.8	8
20	Thermal stability and proton conductivity of densely proton injected phosphate glasses containing rare-earth elements. Journal of Non-Crystalline Solids, 2020, 541, 120064.	1.5	7
21	Quantum dot phosphors free from hazardous elements: Current status and prospects for established materials and new ZnTeâ€based alloys. Journal of the Society for Information Display, 2020, 28, 680-690.	0.8	3
22	Control of the nearâ€surface OH concentration of float glass by anodic proton injection. Journal of the American Ceramic Society, 2020, 103, 3642-3649.	1.9	3
23	Formation of Spherical, Rod- and Branch-Shaped Colloidal In ₂ O ₃ Nanocrystals through Simple Thermolysis of an Oleate Precursor. Materials Transactions, 2020, 61, 462-468.	0.4	2
24	37.2: <i>Invited Paper:</i> Synthesis and optical properties of cadmiumâ€free colloidal II–VI alloy quantum dot phosphor. Digest of Technical Papers SID International Symposium, 2019, 50, 405-405.	0.1	0
25	Transport properties of proton conducting phosphate glass: An electrochemical hydrogen pump enabling the formation of dry hydrogen gas. International Journal of Hydrogen Energy, 2019, 44, 24977-24984.	3.8	8
26	81â€∎: Invited Paper: Quantum Dot Phosphors Containing None of Hazardous Element; ZnTeâ€Based Alloy Quantum Dots. Digest of Technical Papers SID International Symposium, 2019, 50, 1160-1163.	0.1	1
27	Proton transport properties of proton-conducting phosphate glasses at their glass transition temperatures. Physical Chemistry Chemical Physics, 2019, 21, 10744-10749.	1.3	18
28	Tunable Direct Band Gap of β-CuGaO ₂ and β-LiGaO ₂ Solid Solutions in the Full Visible Range. Inorganic Chemistry, 2019, 58, 4262-4267.	1.9	13
29	Fabrication and Morphological Control of Ni-Based Nanowires by Self-Assembled Solution Synthesis. Materials Transactions, 2019, 60, 2188-2194.	0.4	1
30	Comprehensive first-principles study of AgGaO ₂ and CuGaO ₂ polymorphs. Journal of the Ceramic Society of Japan, 2019, 127, 339-347.	0.5	4
31	Fabrication of Au nanoparticles on poly(vinylpyrrolidone) nanowires exhibiting reversible frequency change of localized surface plasmon resonance. AIP Advances, 2018, 8, 015314.	0.6	1
32	Dense proton injection into phosphate glasses using corona discharge treatment. Applied Surface Science, 2018, 428, 718-722.	3.1	6
33	Proton-conducting phosphate glass and its melt exhibiting high electrical conductivity at intermediate temperatures. Journal of Materials Chemistry A, 2018, 6, 23628-23637.	5.2	18
34	Flux growth of \hat{I}^2 -NaGaO2 single crystals. Journal of Crystal Growth, 2018, 504, 26-30.	0.7	4
35	Controlling the electrical conductivity of ternary wurtzite-type and metastable β-AgGaO2 by impurity doping. AlP Advances, 2018, 8, 085203.	0.6	1
36	Catalytic CO oxidation of palladium nanoparticles formed by one-step synthesis on polycarbosilane nanowires. Materials Research Express, 2018, 5, 085003.	0.8	1

#	Article	IF	CITATIONS
37	Colloidal Zn(Te,Se)/ZnS Core/Shell Quantum Dots Exhibiting Narrow-Band and Green Photoluminescence. ACS Omega, 2018, 3, 6703-6709.	1.6	29
38	Design of cadmium-free colloidal II–VI semiconductor quantum dots exhibiting RGB emission. AIP Advances, 2017, 7, .	0.6	22
39	Formation of Au nanoparticle arrays on hydrogel two-dimensional patterns based on poly(vinylpyrrolidone). Japanese Journal of Applied Physics, 2017, 56, 06GG06.	0.8	2
40	Multinary wurtzite-type oxide semiconductors: present status and perspectives. Semiconductor Science and Technology, 2017, 32, 013007.	1.0	10
41	The mobility of proton carriers in phosphate glasses depends on polymerization of the phosphate framework. Physical Chemistry Chemical Physics, 2017, 19, 29669-29675.	1.3	15
42	Formation of Amorphous H ₃ Zr ₂ Si ₂ PO ₁₂ by Electrochemical Substitution of Sodium lons in Na ₃ Zr ₂ Si ₂ PO ₁₂ with Protons. Inorganic Chemistry, 2017, 56, 13949-13954.	1.9	4
43	Synthesis of colloidal Zn(Te,Se) alloy quantum dots. Materials Research Express, 2017, 4, 106501.	0.8	16
44	Variation of crystal structure and optical properties of wurtzite-type oxide semiconductor alloys of β-Cu(Ga,Al)O2. Journal of Applied Physics, 2017, 121, .	1.1	8
45	Fabrication of β-CuGaO2thin films by ion-exchange of β-NaGaO2thin films. Applied Physics Express, 2017, 10, 095501.	1.1	5
46	Wurtzite-Derived Quaternary Oxide Semiconductor Cu ₂ ZnGeO ₄ : Its Structural Characteristics, Optical Properties, and Electronic Structure. Inorganic Chemistry, 2017, 56, 14277-14283.	1.9	6
47	Effect of alkaline-earth species in phosphate glasses on the mobility of proton carriers. Journal of Materials Chemistry A, 2017, 5, 12385-12392.	5.2	14
48	Orientation control of β-NaGaO ₂ thin film: a precursor for β-CuGaO ₂ as a thin-film solar cell absorber. Journal of the Ceramic Society of Japan, 2017, 125, 872-875.	0.5	4
49	First principles calculations of ternary wurtzite \hat{l}^2 -CuGaO2. Journal of Applied Physics, 2016, 119, .	1.1	21
50	Relationship between structure and mobility of proton carriers injected by electrochemical substitution of sodium ions with protons in 35NaO1/2-1 WO3-8NbO5/2-5LaO3/2-51PO5/2-based glasses. Solid State Ionics, 2016, 288, 281-285.	1.3	7
51	High temperature phases with wurtzite-derived structure in Zn2LiGaO4–ZnO alloy system. Journal of Alloys and Compounds, 2016, 688, 69-76.	2.8	4
52	First-Principles Study of CuGaO ₂ Polymorphs: Delafossite α-CuGaO ₂ and Wurtzite β-CuGaO ₂ . Inorganic Chemistry, 2016, 55, 7610-7616.	1.9	29
53	Colloidal semiconductor quantum dots; syntheses, properties and applications. Journal of the Ceramic Society of Japan, 2015, 123, 1-8.	0.5	5
54	Ternary and quaternary wurtzite-type oxide semiconductors: new materials and their properties. , 2015, , .		0

#	Article	IF	CITATIONS
55	Structural and Thermal Properties of Ternary Narrow-Gap Oxide Semiconductor; Wurtzite-Derived β-CuGaO ₂ . Inorganic Chemistry, 2015, 54, 1698-1704.	1.9	33
56	Synthesis of size-controlled colloidal InAs quantum dots using triphenylarsine as a stable arsenic source. Journal of Crystal Growth, 2015, 416, 134-141.	0.7	12
57	Widely bandgap tunable amorphous Cd–Ga–O oxide semiconductors exhibiting electron mobilities ≥10 cm2 Vâ^'1 sâ^'1. Applied Physics Letters, 2015, 106, 082106.	1.5	14
58	Wurtzite-derived ternary l–Ill–O ₂ semiconductors. Science and Technology of Advanced Materials, 2015, 16, 024902.	2.8	23
59	Improving thermal stability and its effects on proton mobility in proton-conducting phosphate glasses prepared by the electrochemical substitution of sodium ions with protons. Solid State Ionics, 2015, 275, 62-65.	1.3	14
60	Structural change of NaO _{1/2} –WO ₃ –NbO _{5/2} –LaO _{3/2} –PO _{5/2induced by electrochemical substitution of sodium ions with protons. Physical Chemistry Chemical Physics, 2015, 17, 13640-13646.})>glass £.3	13
61	Phase separation and crystallization in sodium lanthanum phosphate glasses induced by electrochemical substitution of sodium ions with protons. Physical Chemistry Chemical Physics, 2015, 17, 22855-22861.	1.3	15
62	Structure of β-AgGaO2; ternary l–III–VI2 oxide semiconductor with a wurtzite-derived structure. Journal of Solid State Chemistry, 2015, 222, 66-70.	1.4	18
63	Distribution of Non-Ferrous Metals between Matte and Slag in Copper Matte Smelting of Low Grade Secondary Materials. Journal of MMIJ, 2014, 130, 115-124.	0.4	2
64	Facile synthesis of colloidal InAs nanocrystals using triphenylarsine as an arsenic source. Journal of Crystal Growth, 2014, 405, 39-43.	0.7	2
65	Fabrication of β-AgGaO2 thin films by radio frequency magnetron sputtering. Thin Solid Films, 2014, 559, 112-115.	0.8	11
66	Phase determination of zinc selenide nanocrystals depending on the ligand species of precursor complexes. Journal of Crystal Growth, 2014, 394, 81-88.	0.7	7
67	Wurtzite CuGaO ₂ : A New Direct and Narrow Band Gap Oxide Semiconductor Applicable as a Solar Cell Absorber. Journal of the American Chemical Society, 2014, 136, 3378-3381.	6.6	85
68	Proton conducting tungsten phosphate glass and its application in intermediate temperature fuel cells. Solid State Ionics, 2014, 262, 856-859.	1.3	30
69	Electrochemical substitution of sodium ions with protons in phosphate glass to fabricate pure proton conducting glass at intermediate temperatures. Journal of Materials Chemistry A, 2014, 2, 3940.	5.2	31
70	Electronic transition responsible for size-dependent photoluminescence of colloidal CuInS2quantum dots. Journal of Materials Chemistry C, 2014, 2, 6867.	2.7	60
71	Synthesis of colloidal solution of β-LiGaO ₂ nanocrystals capped with organic surfactant. Journal of the Ceramic Society of Japan, 2014, 122, 195-197.	0.5	1
72	Enhancement by praseodymium addition of catalytic activity of nickel supported on cerium–zirconium oxide in methane steam reforming. Journal of the Ceramic Society of Japan, 2014, 122, 537-542.	0.5	3

#	Article	IF	CITATIONS
73	α-PbO ₂ -related phase appearing in the Sn ^{IV} –Ta–O system transformed from cation-ordered fluorite-related phase. Journal of the Ceramic Society of Japan, 2014, 122, 902-907.	0.5	0
74	Fabrication of ZnF2 thin films and their vacuum ultraviolet transparency. Thin Solid Films, 2013, 534, 508-514.	0.8	7
75	Impact of the Electrical Forming Process on the Resistance Switching Behaviors in Lanthanum-Doped Strontium Titanate Ceramic Chip Devices. Japanese Journal of Applied Physics, 2013, 52, 045802.	0.8	4
76	Electrochemical Substitution of Sodium Ions in Tungsten Phosphate Glass with Protons. Journal of the Electrochemical Society, 2013, 160, E143-E147.	1.3	26
77	Pseudo-binary alloying system of ZnO-AgGaO2 reducing the energy band gap of zinc oxide. Applied Physics Letters, 2013, 103, .	1.5	14
78	Degradation of potential barriers in ZnO-based chip varistors due to electrostatic discharge. Journal of Applied Physics, 2012, 112, 033707.	1.1	8
79	Ultraviolet electroluminescence from colloidal ZnO quantum dots in an all-inorganic multilayer light-emitting device. Applied Physics Letters, 2012, 100, .	1.5	26
80	Structural variation and optical properties of ZnO–LiGaO2 pseudo-binary system. Journal of Solid State Chemistry, 2012, 188, 92-99.	1.4	15
81	Quantum dot phosphors and their application to inorganic electroluminescence device. Thin Solid Films, 2012, 520, 3829-3834.	0.8	17
82	Synthesis of LiGaO2 nanocrystals and their application toward bright UV emission from ZnO quantum dots. Journal of Crystal Growth, 2011, 330, 9-16.	0.7	6
83	UV luminescent organic-capped ZnO quantum dots synthesized by alkoxide hydrolysis with dilute water. Journal of Colloid and Interface Science, 2011, 355, 274-281.	5.0	20
84	Fabrication of ZnO Films Alloyed with LiGaO2by RF-Magnetron Sputtering and Their Optical Property. Japanese Journal of Applied Physics, 2011, 50, 061102.	0.8	6
85	Zn ₂ LiGaO ₄ , Wurtzite-Derived Wide Band Gap Oxide. Japanese Journal of Applied Physics, 2011, 50, 031102.	0.8	13
86	Fabrication of Core–Shell-Type Copper Indium Selenide and Zinc Selenide Composite Quantum Dots and Their Optical Properties. Journal of Nanoscience and Nanotechnology, 2011, 11, 4815-4823.	0.9	13
87	Zn ₂ LiGaO ₄ , Wurtzite-Derived Wide Band Gap Oxide. Japanese Journal of Applied Physics, 2011, 50, 031102.	0.8	15
88	Fabrication of ZnO Films Alloyed with LiGaO ₂ by RF-Magnetron Sputtering and Their Optical Property. Japanese Journal of Applied Physics, 2011, 50, 061102.	0.8	11
89	Extremely Suppressed Grain Growth of Y[sub 2]O[sub 3]-Stabilized Zirconia Nanocrystals Synthesized by the Nonhydrolytic Sol–Gel Technique. Journal of the Electrochemical Society, 2009, 156, K4.	1.3	14
90	Synthesis of Organic Capped Colloidal Zinc Oxide Quantum Dots and Their UV Dominant Emission Property. Materials Research Society Symposia Proceedings, 2009, 1207, 1.	0.1	0

#	Article	IF	CITATIONS
91	Novel wide band gap alloyed semiconductors, x(LiGaO2)1/2-(1â^'x)ZnO, and fabrication of their thin films. Science in China Series D: Earth Sciences, 2009, 52, 111-115.	0.9	7
92	Synthesis of CuInS2 nanocrystals and their structural transformation triggered by ligand exchange. Science Bulletin, 2009, 54, 4005-4008.	1.7	2
93	Colloidal Synthesis of Ternary Copper Indium Diselenide Quantum Dots and Their Optical Properties. Journal of Physical Chemistry C, 2009, 113, 3455-3460.	1.5	112
94	Synthesis of Ternary CulnS ₂ Nanocrystals; Phase Determination by Complex Ligand Species. Chemistry of Materials, 2009, 21, 2607-2613.	3.2	170
95	Size dependent optical band gap of ternary I-III-VI2 semiconductor nanocrystals. Journal of Applied Physics, 2009, 105, .	1.1	172
96	Photoluminescence of CuInS ₂ -based semiconductor quantum dots; Its origin and the effect of ZnS coating. Journal of Physics: Conference Series, 2009, 165, 012028.	0.3	19
97	Cu-Doped Zr-Ce-Pr-O Mixed Oxide Phases with High Oxygen Storage Capacity (OSC). Nippon Kinzoku Gakkaishi/Journal of the Japan Institute of Metals, 2009, 73, 268-274.	0.2	1
98	Zr-Ce-Pr-O Mixed Oxide Phases with High Oxygen Storage Capacity (OSC). Nippon Kinzoku Gakkaishi/Journal of the Japan Institute of Metals, 2009, 73, 262-267.	0.2	1
99	A Cu-added Zr-Ce-Sn-Pr-O mixed oxide phase with a high oxygen storage capacity. Journal of Physics: Conference Series, 2009, 165, 012090.	0.3	0
100	Synthesis of Y ₂ O ₃ -doped CeO ₂ nanocrystals and their surface modification. Journal of Physics: Conference Series, 2009, 165, 012041.	0.3	7
101	Mixed dopant effect in SrZrO3-based proton conductor. Solid State Ionics, 2008, 179, 1116-1119.	1.3	8
102	Formation of Ni ₃ C Nanocrystals by Thermolysis of Nickel Acetylacetonate in Oleylamine: Characterization Using Hard X-ray Photoelectron Spectroscopy. Chemistry of Materials, 2008, 20, 4156-4160.	3.2	162
103	Wide band gap semiconductor alloy: x(LiGaO2)1â^•2–(1â^'x)ZnO. Journal of Applied Physics, 2008, 103, 083706.	1.1	40
104	Nanocrystals of zirconia- and ceria-based solid electrolytes: Syntheses and properties. Science and Technology of Advanced Materials, 2007, 8, 524-530.	2.8	21
105	Chemical role of amines in the colloidal synthesis of CdSe quantum dots and their luminescence properties. Journal of Luminescence, 2007, 126, 21-26.	1.5	56
106	Synthesis of Composite Nanoparticles of Oxide Solid Electrolytes and Their Sintering. Hosokawa Powder Technology Foundation ANNUAL REPORT, 2007, 15, 51-57.	0.0	0
107	Tunable Photoluminescence Wavelength of Chalcopyrite CuInS2-Based Semiconductor Nanocrystals Synthesized in a Colloidal System. Chemistry of Materials, 2006, 18, 3330-3335.	3.2	272
108	Synthesis of CeO[sub 2], ZrO[sub 2] Nanocrystals, and Core-Shell-Type Nanocomposites. Journal of the Electrochemical Society, 2006, 153, A2269.	1.3	12

#	Article	IF	CITATIONS
109	Hydration behavior of Ba2Sc2O5 with an oxygen-deficient perovskite structure. Solid State Ionics, 2006, 177, 2447-2451.	1.3	16
110	Characterization of indium–tin oxide sputtering targets showing various densities of nodule formation. Thin Solid Films, 2006, 503, 22-28.	0.8	46
111	Synthesis of novel cation-ordered compounds with fluorite-related structure prepared by oxidation of Sn–Ta–O pyrochlore. Journal of Solid State Chemistry, 2005, 178, 1254-1261.	1.4	2
112	Infrared study of high temperature proton conducting Sr(Zr0.95M0.05III)O3â^'δ; formation of MIIIO6-cluster depends on dopant species. Solid State Ionics, 2005, 176, 2941-2944.	1.3	15
113	Electrical Conduction Properties of Sr-Doped LaPO4 and CePO4 under Oxidizing and Reducing Conditions ChemInform, 2005, 36, no.	0.1	1
114	Characterization of novel cation-ordered compounds with fluorite and α-PbO2 related structures prepared by oxidation of Sn–Nb–O pyrochlore. Journal of Physics and Chemistry of Solids, 2005, 66, 53-62.	1.9	9
115	Infrared Study of High-Temperature Proton-Conducting Aliovalently Doped SrZrO[sub 3] and BaZrO[sub 3]. Journal of the Electrochemical Society, 2005, 152, E200.	1.3	18
116	Synthesis of CdSe Quantum Dots Using Micro-Flow Reactor and Their Optical Properties. Japanese Journal of Applied Physics, 2005, 44, 452-456.	0.8	10
117	Electrical Conduction Properties of Sr-Doped LaPO[sub 4] and CePO[sub 4] under Oxidizing and Reducing Conditions. Journal of the Electrochemical Society, 2005, 152, A658.	1.3	50
118	Formation and Thermal Stability of Hydrate-Like Compounds of Ba[sub 2](In[sub 1â^'x]M[sup III]x])[sub 2]0[sub 5]â <nh[sub (m[sup="" 152,<br="" 2005,="" 2]0="" and="" electrochemical="" iii]="Ga," journal="" lu,="" of="" sc,="" society,="" the="" y).="">A1068.</nh[sub>	1.3	4
119	O–H stretching vibrations of proton conducting alkaline-earth zirconates. Solid State Ionics, 2004, 168, 99-109.	1.3	41
120	Proton solubility for La2Zr2O7 with a pyrochlore structure doped with a series of alkaline-earth ions. Solid State Ionics, 2004, 167, 389-397.	1.3	50
121	Synthesis of novel compounds with cation ordered fluorite and α-PbO2 related structures by oxidation of Sn2Nb2O7 pyrochlore. Journal of Alloys and Compounds, 2004, 370, 80-89.	2.8	5
122	Photocatalytic behavior of cerium titanates, CeTiO4 and CeTi2O6 and their composite powders with SrTiO3. Journal of Alloys and Compounds, 2004, 376, 262-267.	2.8	61
123	Photocatalytic behavior of titanium oxide-perovskite type Sr(Zr1â^'xYx)O3â^'δ composite particles. Journal of Photochemistry and Photobiology A: Chemistry, 2003, 156, 243-248.	2.0	17
124	Effect of Dopant Species on the Dissolving Site of the Protons in La[sub 2]Zr[sub 2]O[sub 7]-Doped with Alkaline-Earth Ions. Journal of the Electrochemical Society, 2003, 150, E590.	1.3	6
125	Thermodynamic Stability of Metastable Tetragonal t'-Ce0.5Zr0.5O2 Phase in the CeO2-ZrO2 system. High Temperature Materials and Processes, 2003, 22, 157-164.	0.6	4
126	Photodegradation of Methylene Blue Aqueous Solution Sensitized by Pyrochlore-Related κ-CeZrO ₄ Oxide Powder. Materials Transactions, 2003, 44, 1620-1623.	0.4	12

#	Article	IF	CITATIONS
127	Photobleaching of Methylene Blue Aqueous Solution Sensitized by Composite Powders of Titanium Oxide with SrTiO ₃ , BaTiO ₃ , and CaTiO ₃ . Materials Transactions, 2003, 44, 2124-2129.	0.4	23
128	Oxygen release behavior of metastable tetragonal t′meta-(Ce0.5Zr0.5)2 phases prepared by reduction and successive oxidation of t′ phase. Science and Technology of Advanced Materials, 2001, 2, 397-404.	2.8	21
129	Electrical conductivity of metastable κ-CeZrO4 phase possessing ordered arrangement of Ce and Zr ions. Science and Technology of Advanced Materials, 2001, 2, 443-448.	2.8	16
130	Electrical Properties of Proton-Conducting Ca[sup 2+]-Doped La[sub 2]Zr[sub 2]O[sub 7] with a Pyrochlore-Type Structure. Journal of the Electrochemical Society, 2001, 148, E252.	1.3	68
131	Infrared Absorption Spectra of High Temperature Proton Conducting Ca[sup 2+]-Doped La[sub 2]Zr[sub 2]O[sub 7]. Journal of the Electrochemical Society, 2001, 148, E475.	1.3	15
132	Electrical Conductivity of Novel Tetragonal t′meta-(Ce0.5Zr0.5)O2 Phase Prepared by Reduction and Successive Oxidation of t′ Phase. Journal of Solid State Chemistry, 2000, 151, 253-259.	1.4	13
133	Electron trapping center and SnO2-doping mechanism of indium tin oxide. Applied Physics A: Materials Science and Processing, 2000, 71, 609-614.	1.1	17
134	Crystal structure of metastable κ-CeZrO4 phase possessing an ordered arrangement of Ce and Zr ions. Journal of Alloys and Compounds, 2000, 312, 94-103.	2.8	124
135	Vibrational Spectroscopic and X-Ray Diffraction Studies of Cerium Zirconium Oxides with Ce/Zr Composition Ratio=1 Prepared by Reduction and Successive Oxidation of t′-(Ce0.5Zr0.5)O2 Phase. Journal of Solid State Chemistry, 1999, 147, 573-583.	1.4	110
136	Oxygen Release Behavior of CeZrO4Powders and Appearance of New Compoundsl̂ºand t*. Journal of Solid State Chemistry, 1998, 138, 47-54.	1.4	114
137	Properties of transition metal oxides with layered perovskite structure. Solid State Ionics, 1998, 108, 255-260.	1.3	6
138	Oxygen release behaviour of Ce(1â°'x)ZrxO2 powders and appearance of Ce(8â°'4y)Zr4yO(14â^'Î′) solid solution in the ZrO2–CeO2–CeO1.5 system. Journal of Alloys and Compounds, 1998, 270, 107-114.	2.8	66
139	Thermodynamic Behavior of Various Phases Appearing in the CeZrO4 â€â€‰CeZrO3.5 System and the Formation of Metastable Solid Solutions. Journal of the Electrochemical Society, 1998, 145, 1406-1413.	1.3	37
140	High Efficiency-Carrier-Generation for the Oxygen Release Reaction in Indium Tin Oxide. Japanese Journal of Applied Physics, 1998, 37, L879-L881.	0.8	11
141	In-SituObservation of the Electrical Conductivity upon Release and Uptake of Oxygen in Indium Tin Oxide Sinter. Japanese Journal of Applied Physics, 1998, 37, 868-871.	0.8	9
142	Observation of Electronic Structure in Conduction Band of CaTiO ₃ . Journal of the Ceramic Society of Japan, 1998, 106, 964-967.	1.3	6
143	DC electrorheology of fluid suspending barium titanate in the range of ferroelectric size effects. Ferroelectrics, 1997, 203, 241-248.	0.3	2
144	New mixed-valence oxides of bismuth: Bi1â^'xYxO1.5+δ (x=0.4). Journal of Materials Chemistry, 1997, 7, 943-946.	6.7	20

#	Article	IF	CITATIONS
145	Water and hydrogen evolution properties and protonic conducting behaviors of Ca2+-doped La2Zr2O7 with a pyrochlore structure. Solid State Ionics, 1997, 104, 249-258.	1.3	57
146	Optical absorption spectra and the nature of conduction carriers of hole-doped Sr1+xLa1â^'xFeO4. Solid State Communications, 1996, 97, 411-415.	0.9	5
147	Features of valence band structure of. Journal of Physics Condensed Matter, 1996, 8, 303-312.	0.7	7
148	Preparation and Electrical Properties of La _{2-<i>x</i>} Sr _{<i>x</i>} MnO _{4+Î} with K ₂ NiF ₄ -Structure. Journal of the Ceramic Society of Japan, 1995, 103, 1297-1301.	1.3	5
149	Electronic Transport Properties of Hole-Doped Sr _{1+<i>x</i>} La _{1-<i>x</i>} CrO _{4+Î′} . Journal of the Ceramic Society of Japan, 1995, 103, 1112-1116.	1.3	0
150	New Oxide Phase \$f Cd_{2(1-{inmbi x})}Y_{2{inmbi x}Sb_{2}O_{7}\$ Pyrochlore with a Wide Band Gap and High Electrical Conductivity. Japanese Journal of Applied Physics, 1994, 33, L238-L240.	0.8	13
151	Preparation of Cd1â^xYxSb2O6thin film on glass substrate by radio frequency sputtering. Applied Physics Letters, 1994, 65, 406-408.	1.5	39
152	Electrical and magnetic properties of hole-dopedSr1+xLa1â^'xFeO4. Physical Review B, 1994, 49, 10194-10199.	1.1	28
153	Electronic structure of hole-dopedSr1+xLa1â^'xFeO4studied by UPS and XAS. Physical Review B, 1994, 49, 10200-10205.	1.1	9
154	Generation of electron carriers in insulating thin film of MgIn2O4spinel by Li+implantation. Journal of Applied Physics, 1994, 76, 7935-7941.	1.1	90
155	New ultravioletâ€ŧransport electroconductive oxide, ZnGa2O4spinel. Applied Physics Letters, 1994, 64, 1077-1078.	1.5	214
156	Preparation of oxygen excess SrLaFeO4+ \hat{l} and its electrical and magnetic properties. Solid State Communications, 1993, 88, 807-811.	0.9	24
157	New oxide phase with wide band gap and high electroconductivity CdGa2O4spinel. Applied Physics Letters, 1993, 62, 499-500.	1.5	79
158	Preparation of MgIn2O4-XThin Films on Glass Substrate by RF Sputtering. Japanese Journal of Applied Physics, 1993, 32, L1260-L1262.	0.8	65
159	New oxide phase Cd1â^'xYxSb2O6with a wide band gap and high electrical conductivity. Applied Physics Letters, 1993, 63, 3335-3337.	1.5	17
160	New oxide phase with wide band gap and high electroconductivity, MgIn2O4. Applied Physics Letters, 1992, 61, 1954-1955.	1.5	128